Q. J. R. Meteorol. Soc. (1990), **116**, pp. 221–238 551.577.38:551.577.35(66)

Onset of Sahelian drought viewed as a fluctuation-induced transition

By G. R. DEMAREE
Koninklijk Meteorologisch Instituut van België, Ringlaan 3, B-1180 Bruxelles, Belgium
and
C. NICOLIS
Institut d'Aéronomie Spatiale de Belgique, Avenue Circulaire 3, B-1180 Bruxelles, Belgium

(Received 14 July 1988; revised 27 June 1989)

SUMMARY

A statistical analysis of representative sets of rainfall data in the west Sahel region is performed and a jump transition in the late sixties is detected. It is suggested that the main features associated with the record can be accounted for by a fluctuation-induced transition between two stable precipitation regimes: a 'humid' and a 'dry' state. A minimal model involving the dominant nonlinearities is constructed and its parameters determined from the data. An attempt is made to arrive at a statistical prediction of the duration of the alternate regimes through the relative stability of the two stable states as deduced from mean values and higher moments of residence times. The behaviour predicted by the model is in good qualitative agreement with the record.

1. INTRODUCTION

Since its onset in the late sixties, the catastrophic drought that ravaged the west African Sahel has attracted widespread interest (see e.g. Hare 1983). This major climatic event is characterized by (a), a strong persistence, about two decades; (b) a spatial range extending over the whole sub-Saharan region; and (c), a nearly synchronous occurrence of similar events in the subtropics of southern Africa (Lamb 1982, 1983, 1985; Nicholson and Chervin 1983; Nicholson 1989).

The current drought is far from being a unique event. During the present century the Sahelian region experienced several periods of dry conditions of varying duration, magnitude and spatial extent (Grove 1973; Sircoulon 1976). Looking even further in the past, it appears that during at least the last five centuries rainfall fluctuations of extremely variable duration (from years to several decades) have also occurred (Nicholson 1978).

For a long time it was thought that the Sahelian precipitation regime could be interpreted as a random succession of dry and wet periods of a stationary rainfall process (see e.g. Bunting *et al.* 1976; Landsberg 1975; Glantz and Katz 1985, 1986). In recent years however, growing evidence of the non-stationary character of the annual rainfall amounts recorded at Sahelian stations has become available. Snijders (1986) reported evidence of non-stationarity of a Burkina Faso areal rainy season precipitation index over the reference period 1953–1983. Hubert and Carbonnel (1987), who studied long-term annual precipitation series from 42 stations spread over the Sahel, and Demarée and Chadilly (1988), who analysed one representative station, arrived at the same conclusion. Common to the above-mentioned studies is the major finding of an *abrupt* change in precipitation in the form of a more or less well defined jump in the mean, preceded and followed by an otherwise stationary pattern of events.

In this paper we develop the thesis that Sahelian drought is a recurrent aperiodic event related to ongoing transitions between a stable state of 'quasi-normal' rainfall and a stable state of low rainfall. We first report in section 2 on the statistical analysis of two representative time series: the 1904–1987 rainfall record at the Kaédi station in Mauritania and the 1941–1986 areal-averaged precipitation index computed by Lamb and based on the analysis of 14–20 sub-Saharan stations (1985, and personal note 1988). This leads us to conclude that a jump transition has indeed occurred, and to identify the main features (mean precipitation and variance) of the two 'states' before and after the transition. Concomitantly, we show that the data points are not normally distributed. Instead, they are fitted to a good approximation by a bimodal distribution in the form of two slightly overlapping Gaussians. In section 3 we review, from the standpoint of the theory of dynamical systems, the scenarios that could possibly give rise to the observed behaviour. We conclude that the most plausible scenario is a series of intermittent jumps between two stable states available simultaneously to the underlying dynamical system. These 'hydrological transitions' between humid and dry regimes are triggered by stochastic forcings (fluctuations) to which the system is inevitably subjected. In section 4 we introduce the simplest possible model compatible with the above dynamical scenario. It involves a single variable, a cubic nonlinearity and a white-noise forcing term. We show that the model actually includes the dominant nonlinearities that are likely to be present, and constitutes therefore the canonical form of the precipitation regime in the presence of bistability. The connection of the conceptual model thus obtained with the physical mechanisms likely to take part in the hydrology of the Sahelian region is attempted. Furthermore, we show how the parameters involved can be determined from the data. We subsequently derive, in section 5, the relative stability of the states in the presence of fluctuations. It is found that the time spent by the system around each of the states (residence time) is subject to a strong variability. This conclusion is qualitatively speaking in agreement with the record. The implications of our approach to the problem of predictability of these events are discussed in section 6.

2. Data and statistical analysis

In this section we perform a statistical analysis of annual rainfall records from the beginning of the present century until 1987. We first use the time series from the Kaédi station situated in Mauritania on the right bank of the Senegal River. Although there are some gaps in the station record, there is convincing evidence that Kaédi is quite representative of the precipitation regime of the west Sahel region. Indeed, comparing the time evolution of rainfall with other stations one realizes that although regional quantitative differences may exist, the overall shape and the recently observed global shift of the long-term average are similar (see for instance Farmer and Wigley 1985, pp. 58 and 64). The Kaédi rainfall data, expressed in annual rainfall amounts and in standard deviation departures from the long-term station average, are given in Figs. 1(a) and (b), respectively. The most striking feature is the negative shift of the long-term average for almost the entire 1968–1987 period.

We first analyse the stationarity of the record. To this end we apply the non-parametric Mann–Kendall–Sneyers test, based on the computation of Mann's rank statistic (Kendall and Stuart 1979; Sneyers 1975). Let $x_1, \ldots, x_n$ be the data points. For each element x_i the numbers n_i of elements x_j preceding it ($j < i$) such that $x_j < x_i$ are computed. Under the null hypothesis (no trend) one then shows that the test statistic

$$t_k = \sum_{i=1}^{i=k} n_i \tag{1}$$

is normally distributed, with mean and variance given by

$$\bar{t}_k = E(t_k) = k(k-1)/4; \qquad \overline{\delta t_k^2} = \mathrm{var}(t_k) = k(k-1)(2k+5)/72. \tag{2}$$

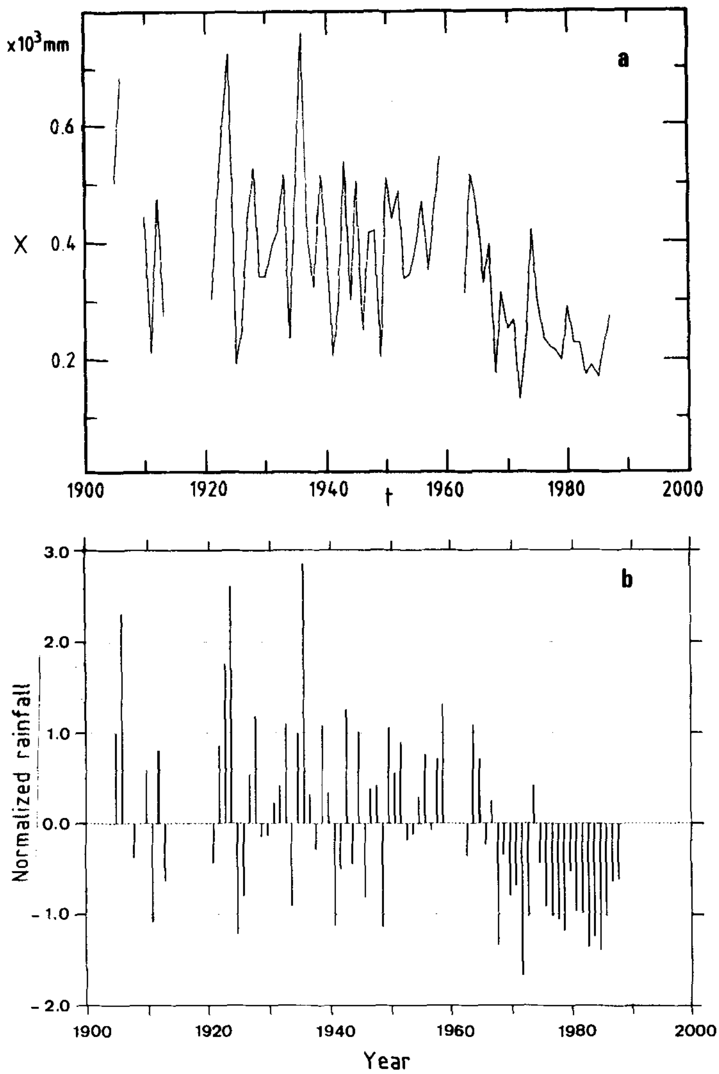

Figure 1. (a) Yearly precipitation amounts at Kaédi (Mauritania), reference period 1904–1987. (b) Normalized rainfall departures, in standard deviations, for the time series of Fig. 1(a).

Let

$$u_k = (t_k - \bar{t}_k)/(\overline{\delta t_k^2})^{1/2} \tag{3}$$

be the normalized variable; the probability α_1

$$\alpha_1 = \text{prob}(|u| > |u_k|) \tag{4}$$

is then calculated. If α_0 is the significance level of the test (e.g. $\alpha_0 = 0{\cdot}05$), the null hypothesis is accepted or rejected according to whether $\alpha_1 >$ or $< \alpha_0$. When values of u_k leading to violation are significant, the existence of an increasing trend ($u_k > 0$) or a decreasing trend ($u_k < 0$) in the data will be indicated. The sequential version of the test used here enables detection of the approximate time of occurrence of the trend by locating the intersection of the direct and backward curves of the test statistic, if it occurs within the confidence interval.

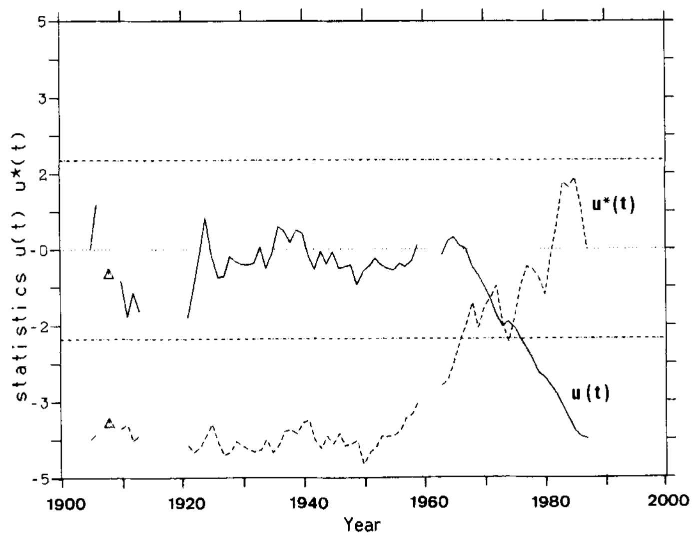

Figure 2. Mann–Kendall–Sneyers sequential trend test of the time series of Fig. 1(a): for forward (u_k, full line) and backward (u_k^*, dashed line) time series. The horizontal dashed-dotted lines represent the critical values corresponding to the 5% significance level.

The Mann–Kendall–Sneyers test, applied to the annual rainfall amounts over the reference period 1904–1987, shows a highly significant *downward* trend. Figure 2 shows graphically the forward (u_k, full line) and backward (u_k^*, broken line) applications of the test; the horizontal dotted lines indicate the two-sided 95% confidence interval; missing years are omitted. Since the direct and the backward curves of the test statistic do not leave the 95% confidence interval over the period 1904 until the end of the sixties, as well as over the period from the end of the sixties until 1987, the null hypothesis of no trend cannot be rejected for the two periods separately on the basis of this test. Furthermore, since the intersection of these two curves lies in the above confidence interval one may reasonably conclude that the transition is abrupt (Goossens and Berger 1987).

Our next objective is to localize more sharply the time of the transition. To this end a change-point test was applied to the same precipitation data. The non-parametric Pettitt's change-point test (Pettitt 1979), which enables the detection of a once-occurring jump in the mean at an unknown time, was selected. The test statistic is

$$K_N = \max_{1 \leq t \leq N} |U_{t,N}| \tag{5}$$

where the statistic $U_{t,N}$ is equivalent to a Mann–Whitney test statistic for testing that two samples

$$X_1, X_2, \ldots, X_\tau \qquad \text{and} \qquad X_{\tau+1}, \ldots, X_N \tag{6}$$

are from the same population. The statistic U counts the number of times a member of the first sample exceeds a member of the second sample. It was shown that the maximum value of K_N, which corresponds to the change-point, is attained for the year 1967; the approximate significance probability (Pettitt 1979) associated with this value is 0·00005, strong evidence of an abrupt change in the mean. Figure 3 gives a graphical representation of the statistic $U_{t,N}$, including the approximate significance probabilities at the 5% and

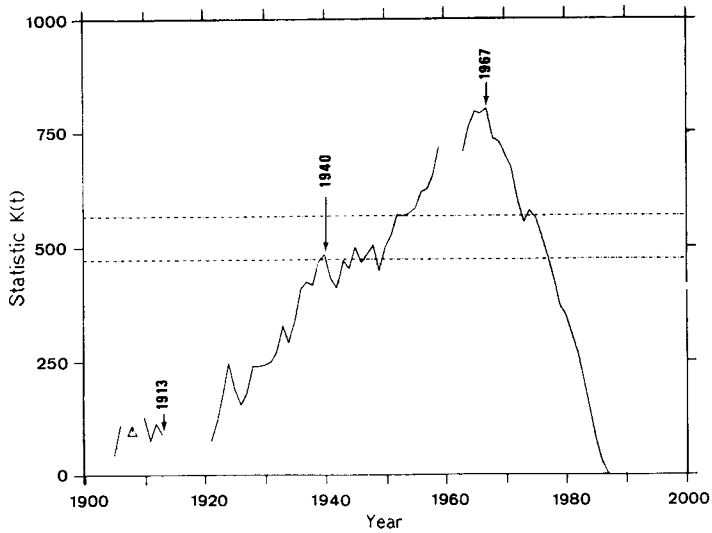

Figure 3. Pettitt's test for detecting a shift in the mean of the time series of Fig. 1(a). The horizontal lines show the approximate significance probabilities at the 5% and 1% levels. The maximum corresponds to the change-point; the dry periods labelled 1913 and 1940 are indicated as well.

1% levels of significance. Notice the sharpness of the maximum, which further reflects the abruptness of the transition.

A similar conclusion of an abrupt transition in the mean around the late sixties has recently been reported from the analysis of a Burkina Faso precipitation index (Snijders 1986) and of 42 series spread over the Sahel, from Sénégal through Nigeria (Hubert and Carbonnel 1987).

Numerical values for means, standard deviations (rounded to the nearest integer) and coefficients of variation for the two considered periods for Kaédi are given in Table 1(a). *A posteriori* application of Student's difference test for the mean, assuming unequal variances, results in the rejection of the hypothesis of equal means at the 0·01% level of significance. The same conclusion is obtained for the variances by the classical F-test. Deviations from the normal distribution assumption may bias the application of Worsley's parametric change-point test (see Buishand 1982, 1984). For that reason the non-parametric Pettitt's test was chosen. Further examination of the record reveals that the decrease of the variance shown in Table 1(a) occurs in time in a more or less monotonic fashion. In particular, no increase is observed in the vicinity of the transition.

We now comment on the statistical distribution of the data points. Computation of the chi-square goodness-of-fit index allows us to accept the hypothesis that both samples of annual precipitation data for the separate periods are normally distributed, but with significantly different means and variances in accordance with the above conclusions. Alternatively, the hypothesis that the entire sample consists of a single normal distribution is rejected at the 5% significance level. This is in good agreement with the idea of nonstationarity of the overall time series and of the possibility of two distinct precipitation regimes. Figure 4 depicts a probability plot—a plot of a magnitude v. a probability—of the two samples: full lines represent the estimated Gaussians (on probability paper); crosses and plusses, the data points of the two samples respectively; and dotted lines the corresponding 95% confidence interval for the estimated value of the observed variable. The agreement is quite satisfactory especially if one considers the limited number of records involved.

TABLE 1. STATISTICS OF MEAN ANNUAL PRECIPITATION RECORD

(a)

Kaédi	Period 1904–1967	Period 1968–1987
Number of records (years)	51	20
Mean (mm)	413	236
Standard deviation (mm)	130	64
Coefficient of variation	0·315	0·272

(b)

Lamb's Index	Period 1941–1967	Period 1968–1986
Number of records (years)	27	19
Mean	0·307	−0·689
Standard deviation	0·485	0·440
Coefficient of variation	1·58	0·638

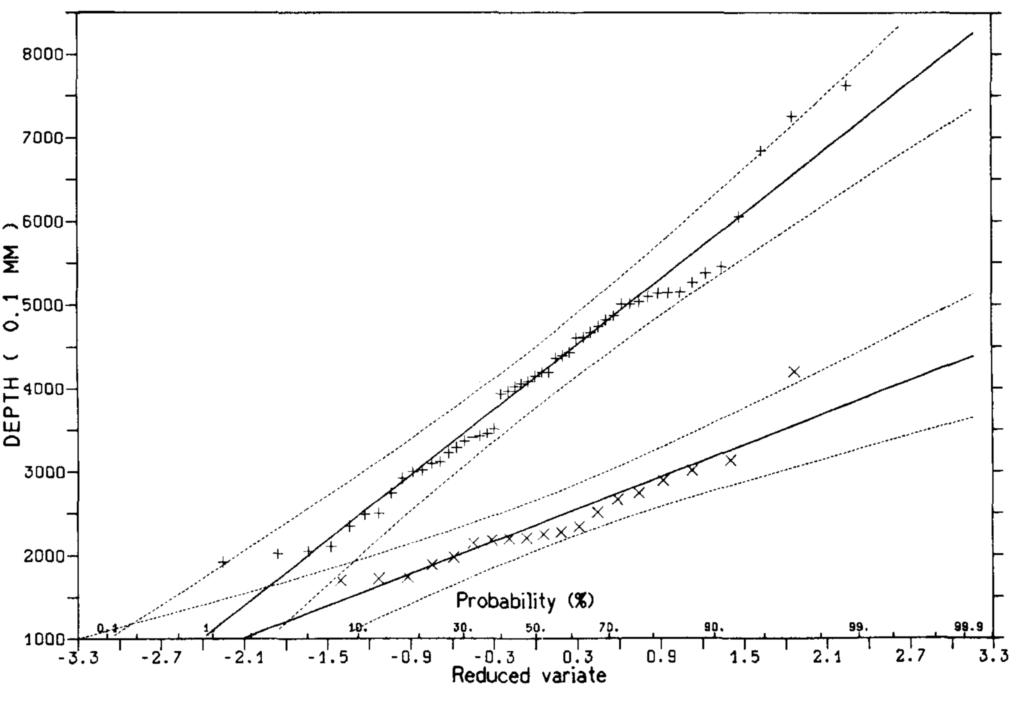

Figure 4. Probability plot of the normal distributions adjusted to the two samples consisting of the annual rainfall data preceding and following the detected climatic shift.

In order to show that the above conclusions are not a peculiarity related to the local dynamics around the Kaédi area we have complemented them with a similar analysis of an areal-averaged precipitation index computed by Lamb (1985, and personal note 1988) for the period 1941–1986. Figure 5(a) depicts the record of suitably normalized April-October rainfall departures from the global time average for 14 to 20 sub-Saharan stations. The Mann–Kendall–Sneyers sequential test for randomness against trend (Fig. 5(b)) shows once more a highly significant downward trend. Application of Pettitt's change-level test (Fig. 5(c)) allows us to locate this shift in the mean in 1967–1968. Table 1(b) summarizes the results of the statistical analysis. In summary, the analysis of Lamb's

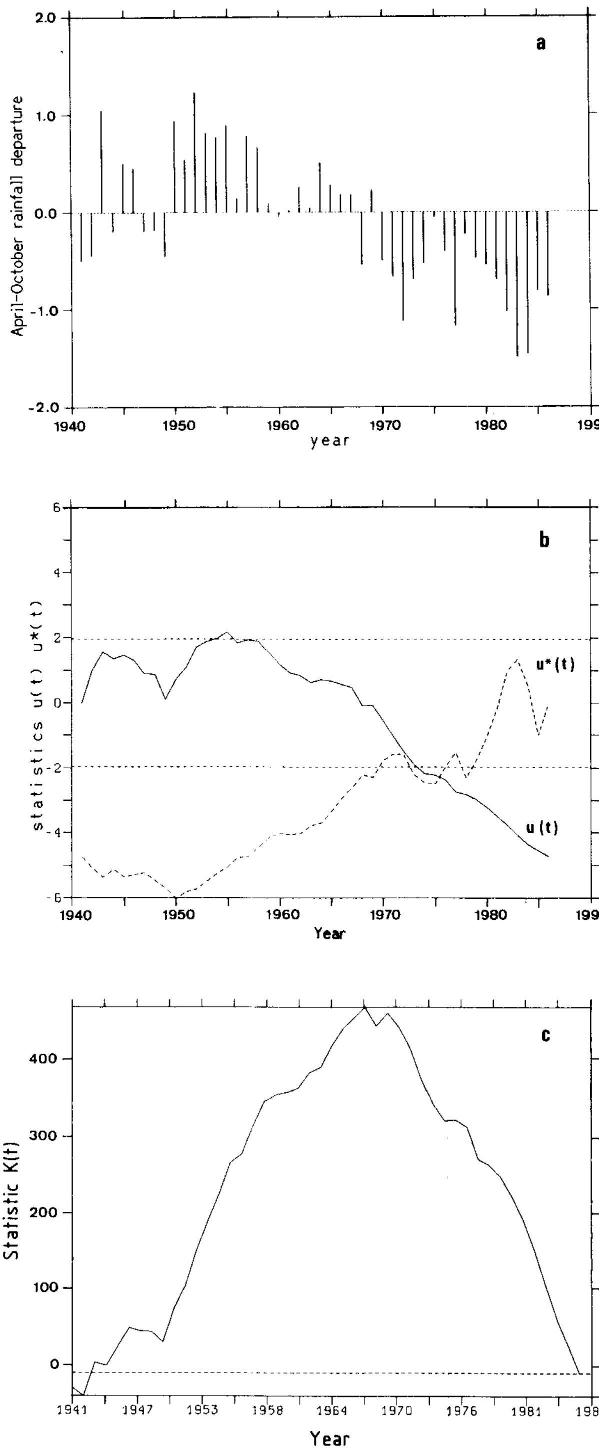

Figure 5. (a) Time series of Lamb's regional precipitation index for the western Sahel. (b) and (c) As in Figs. 2 and 3 but for the data shown in (a).

index leads to similar conclusions as the analysis of the Kaédi station record. This adds extra credence to the view that the western Sahel precipitation regime underwent in the late sixties a sharp transition from a quasi-normal to a dry state. Note, however, that a quantitative comparison cannot be made since Lamb's index is the result of a complex (nonlinear) normalization procedure.

3. Dynamical scenarios suggested by the data

We have demonstrated the non-stationary character of the data analysed in section 2, and the occurrence of a well-defined transition point. Our ultimate goal is to build a mathematical model capturing these two essential features of the record, and to develop a method for making predictions about future trends. Before we go to this subject, however, we present in this section a critical analysis of the type of model that is likely to be relevant in this context.

The most common classes of model used to describe variability of climatic time series are linear autoregressive models. Let X be the variable associated with the record, $\overline{X}$ its long-term average. Defining

$$x = X - \overline{X} \tag{7a}$$

one then writes (see e.g. Box and Jenkins 1976) an equation for the evolution of x of the form

$$dx/dt = -\lambda x + F(t). \tag{7b}$$

In this equation the parameter λ accounts for the mechanisms by which an instantaneous deviation of X from the reference value $\overline{X}$ decays in time. Its inverse, λ^{-1}, plays the role of relaxation or persistence time of the disturbance. Finally, $F(t)$ stands for a *stochastic forcing*. Such a forcing may reflect the random imbalances that inevitably exist between the various internally generated processes, such as transport or radiative mechanisms. It may also reflect random disturbances of external origin acting on the system. Ordinarily, $F(t)$ is modelled as a Gaussian white noise:

$$\langle F(t)\rangle = 0 \qquad \langle F(t)F(t')\rangle = q^2\delta(t-t') \tag{8}$$

where q^2 is the variance and $\delta(t)$ is the Dirac delta function.

Suppose first that λ remains constant in time. Equations (7)–(8) describe then a stationary process characterized by a random succession of fluctuations around a well-defined mean (here $\bar{x} = 0$) whose statistical description is given by a single humped Gaussian. Both these features are in disagreement with the analysis of the record performed in section 2. This class of model has therefore to be ruled out.

Suppose next that the model parameter λ is variable. For example, one may argue that λ varies in a stepwise fashion from a value representative of a period of weak persistence to a value representative of a period of high persistence. It is easy to convince oneself that this will not modify the two main aspects that characterized the response of the variable x in the case of fixed λ, namely the existence of a well-defined mean ($\bar{x} = 0$) and of a single humped Gaussian distribution. The only difference between the two cases will be that the fluctuations of x will be more correlated in the high persistence than in the low persistence regime. This model must therefore also be dismissed on the basis of the record. More generally, as long as the reference state remains stable ($\lambda > 0$) the response is bound to share the above-mentioned features, which are in disagreement with the record.

Let us now turn to a new possibility. We stipulate that in the course of the variation of the parameter λ the nonlinearities that were initially neglected in Eq. (7b), begin to play an important role. This cannot happen in the range of stability of x ($\lambda > 0$), but it will be manifested as soon as λ crosses zero. At this point Eq. (7b) will lead to exponential explosion, but the nonlinearities will saturate this explosive behaviour and will eventually lead to a new branch of solutions, $\bar{x} \neq 0$. This is the phenomenon of *bifurcation*, which is of central importance in the theory of dynamical systems (Nicolis and Prigogine 1977).

To what extent is this scenario acceptable? Let us first remark that it does share some of the features of the record, in particular the transition between two different stable states. On the other hand, it is well known (Nicolis and Prigogine 1977; Nicolis 1988) that in a noisy system the passage through a bifurcation is manifested by strong fluctuations, which should lead to the enhancement of the variance. This is different from the result obtained in the preceding section on the basis of our data set. As a consequence, the above scenario is to be ruled out.

Having excluded the possibility of fluctuations around a well-defined reference (steady) state and the bifurcation of new states in a noisy environment, we now turn to a final possibility: namely, fluctuation-induced intermittent (aperiodic) transitions between co-existing steady states. Qualitatively speaking, the view that there should be *bimodality* in the Sahelian hydrological system seems to be compatible with the jump in mean observed in the record. In addition, it does not exclude *a priori* a downward trend in the variance of the fluctuations. As we show in this and in the following section, one can sharpen this compatibility further and determine from the data most of the parameters involved in the mathematical formulation.

We first present a conceptual model of transitions between alternative steady states. Let, as before, x be a state variable such as the average annual precipitation amount. We again decompose the time evolution of x into two contributions, according to (Hasselmann 1976; Nicolis and Nicolis 1981; Sutera 1981)

$$dx/dt = f(x, \lambda_o) + F(t). \tag{9}$$

Contrary to Eq. (7b), the systematic part of the evolution f, including the effect of feedbacks, of radiation and of the parameters (λ_o) built in the system, is here a nonlinear function of x. As regards the stochastic forcing $F(t)$, as discussed earlier, it represents internal fluctuations arising from random imbalances or random disturbances of external origin. A relevant example of the latter is provided by sea surface temperature (s.s.t.) anomalies whose possible role in the present context has been suggested by Folland *et al.* (1986). As in Eq. (8) $F(t)$ is assumed to define a Gaussian white noise process.

The existence of two alternative steady states will be reflected in the structure of the function $f(x, \lambda_o)$ through the requirement that the equation

$$f(x_0, \lambda_o) = 0 \tag{10}$$

has several solutions for the same values of λ_o. This of course can be the case only if f is a nonlinear function of x. In a sense, therefore, our conceptual model, Eq. (9), may be viewed as a nonlinear regression model for interpreting the data.

For convenience we introduce the 'kinetic potential' $U(x, \lambda_o)$ through the relation (Nicolis and Nicolis 1981; Sutera 1981)

$$U = -\int f(x, \lambda_o)dx \tag{11}$$

and cast Eq. (9) in the form

$$dx/dt = -\partial U/\partial x + F(t). \tag{12}$$

Equation (12) is a stochastic differential equation defining a continuous Markov process $x(t)$. It is well known (Gardiner 1983) that the probability density $P(x,t)$ for having a value x of the state variable at time t is given by the Fokker–Planck equation (we set $U' = \partial U/\partial x$):

$$\frac{\partial P(x,t)}{\partial t} = \frac{\partial(U'P)}{\partial x} + \frac{q^2}{2}\frac{\partial^2 P}{\partial x^2}. \tag{13}$$

The steady-state solution of this equation, $P_s(x)$, is easily found to be

$$P_s(x) = Z^{-1}\exp[-(2/q^2)U(x)] \tag{14a}$$

where the normalization factor Z is given by

$$Z = \int_D \exp[-(2/q^2)U(x)]\,dx \tag{14b}$$

D being the domain of variation of x.

Our next task is to analyse the structure of the nonlinear function f, of the potential U and of the stationary probability P_s on the basis of the information contained in the data.

4. The cubic model

The simplest version of the model of the previous section compatible with the data corresponds to a cubic precipitation law $f(x, \lambda_0)$. Indeed, besides admitting under suitable conditions two stable steady states, such a law can generate a third unstable steady state separating the two stable ones. This is a necessary condition for satisfying such requirements as the boundedness of solutions of the dynamical system. Actually, as we shall see later in this section, as long as the number of stable states is equal to two the cubic model contains all relevant nonlinearities, in the sense that additional, higher-order, terms can generate only small corrections.

Arguing first in terms of suitably reduced variables, parameters and time scale τ we write Eq. (9) in the absence of fluctuations in the more explicit form

$$d\bar{x}/d\tau = -\bar{x}^3 + \lambda\bar{x}^2 - \mu\bar{x} + \nu. \tag{15a}$$

Here $\bar{x}$ denotes the 'deterministic' (fluctuation-free) part of x. The minus sign in front of $\bar{x}^3$ ensures global boundedness of the solutions, and λ, μ, ν are three parameters related to the three steady-state solutions a, b, c through

$$\lambda = a + b + c, \qquad \mu = bc + ca + ab, \qquad \nu = abc. \tag{15b}$$

The corresponding potential U in Eq. (11) is now given (up to a constant) by

$$U(\bar{x}) = \bar{x}^4/4 - \lambda\bar{x}^3/3 + \mu\bar{x}^2/2 - \nu\bar{x}. \tag{16}$$

Obviously, the stable solutions (say, a and c) correspond to the minima of U, whereas the unstable one (b) corresponds to the maximum. In the absence of fluctuations the system will settle on one of the two minima of the potential. But in a noisy environment, there will be sooner or later fluctuation-induced jumps between a and c, whose characteristic time will depend on the noise strength q^2 (Eq. (8)) and on the system's parameters (see e.g. Gardiner 1983).

Let us comment on the physical interpretation of the various terms of (15a). Since a cubic can always be transformed to a 'canonical' form free of quadratic terms, we are essentially dealing with a rate function of the form

$$u + v\bar{y} - \bar{y}^3 \tag{17}$$

where u and v are combinations of the initial parameters and $\bar{y}$ is the transformed variable. The connection with the various mechanisms involved in the dynamics of deserts is the following: u can be thought of as an input term, and $v\bar{y}$ as a positive feedback of rainfall into itself. For instance, following the hypothesis of Otterman (1974) and Charney (1975) this feedback would operate through a change of the albedo of the ground. Although the specific mechanisms by which the albedo is changed are not yet clear (see e.g. Oguntoyinbo 1986 and references therein) for our purposes we keep in mind that the linear term in Eq. (17) represents an overall effect of precipitation on itself. Finally, $-\bar{y}^3$ is a nonlinear restoring mechanism whose origin cannot be specified further at this level of description, but requires a more detailed meteorological study.

Summarizing then, we have from (15) and (16) on the one side and from (9) and (13) on the other side the explicit form of the Fokker–Planck equation and of the corresponding stochastic differential equation

$$\frac{\partial P}{\partial \tau} = \frac{\partial}{\partial x}[x^3 - \lambda x^2 + \mu x - \nu]\, P + \frac{q^2}{2}\frac{\partial^2 P}{\partial x^2} \tag{18}$$

and

$$dx/d\tau = -x^3 + \lambda x^2 - \mu x + \nu + F(\tau). \tag{19}$$

Our next task is to specify, as far as possible, the model parameters on the basis of the data. From the discussion of section 2 it is clear that what we have mainly at our disposal are static quantities such as the means and variances on the two sides of the transition. As regards time-dependent properties it should first be realized that in the problem at hand two kinds of time scales are involved. A 'deterministic' one, associated with relaxation phenomena around each of the minima of the potential, and a 'stochastic' one, associated with the fluctuation-induced transitions between the two minima. The former can be related to the system's parameters as follows. We linearize the equation of evolution in the absence of fluctuations around one of the stable states, say c, by setting

$$x = c + \delta x, \qquad |\delta x/c| \ll 1. \tag{20}$$

One obtains in this way

$$d\,\delta x/d\tau = -U''(c)\delta x. \tag{21}$$

Or, substituting $\tau = \rho t$ where τ is the reduced time used so far and t the real time

$$d\,\delta x/dt = -\rho U''(c)\delta x. \tag{22}$$

Obviously, $\rho U''(c)$ plays the role of an inverse relaxation time. Now, as pointed out by Kraus (1977), the spectra of precipitation data from many arid regions have a dominant maximum centred on a frequency corresponding to a time of 10 years or more. We shall therefore use this result to fix the deterministic time scale of our problem by requiring $[\rho U''(c)]^{-1}$ to be equal to this value.

As for the second time scale we shall see in section 5 that it will come out as a natural consequence of our model. Moreover, it will be possible to determine the relative properties of the two stable states independently of the scaling parameter ρ.

Turning now to the more quantitative aspects, we begin by exploring the data referring to static properties. Requiring that the mean values of the two plateaux before and after the transition be identical to the two stable states a and c of our model, yields (cf. Table 1(a)) $a = 0{\cdot}413\,\mathrm{m}$, $c = 0{\cdot}236\,\mathrm{m}$.

We next explore the information contained in the variances. Multiplying Eq. (18) by x^2 and integrating over x we obtain

$$\tfrac{1}{2}d\langle x^2\rangle/d\tau = -\langle U'x\rangle + q^2/2. \tag{23}$$

Because of the nonlinearity in U', Eq. (23) is not closed: the right-hand side involves higher moments such as $\langle x^3\rangle$ and $\langle x^4\rangle$, in addition to the second moment $\langle x^2\rangle$. Nevertheless, keeping in mind the statistical analysis of section 2, we can circumvent this difficulty by linearizing successively around the two states a and c and approximating each of the two peaks by a Gaussian centred on the local maximum. Setting as before (see Eq. (20))

$$x = x_0 + \delta x, \qquad |\delta x/x_0| \ll 1 \tag{24}$$

x_0 being a or c, Eq. (23) then gives rise to the following two relations

$$\frac{1}{2}\frac{d}{d\tau}\langle\delta x^2\rangle_a = -U''_a\langle\delta x^2\rangle_a + \frac{q^2}{2} \tag{25a}$$

$$\frac{1}{2}\frac{d}{d\tau}\langle\delta x^2\rangle_c = -U''_c\langle\delta x^2\rangle_c + \frac{q^2}{2} \tag{25b}$$

where the subscripts 'a' and 'c' indicate the state on which the corresponding quantity is to be evaluated. The solution of Eqs. (25) at the steady state yields

$$\langle\delta x^2\rangle_a = q^2/2U''_a, \qquad \langle\delta x^2\rangle_c = q^2/2U''_c. \tag{26}$$

This is a system of two equations for the two unknowns b and q^2, contained in U, in addition to a and c already determined. Using Eq. (19), the explicit form of U (Eq. (16)), as well as the values of the variances around a and c inferred from section 2, we obtain: $b = 0{\cdot}378\,\mathrm{m}$, $q^2 = 2{\cdot}07\times10^{-4}\mathrm{m}^2\mathrm{y}^{-1}$. Combining with Eq. (15b) we can identify the model parameters λ, μ, ν to be

$$\lambda = 1{\cdot}03, \qquad \mu = 0{\cdot}343, \qquad \nu = 3{\cdot}69\times10^{-2}. \tag{27}$$

Finally, the parameter ρ is specified by the equality (cf. Eq. (22))

$$[\rho U''(c)]^{-1} \approx 10\,\mathrm{y}$$

or, using the above values of λ, μ, ν,

$$\rho \approx 16\,\mathrm{y}^{-1}. \tag{28}$$

We have now at our disposal the parameters determining the full form of the potential (Eq. (16)). Figure 6(a) depicts its dependence on the variable x. We obtain a double-well potential, which substantiates the idea of two co-existing time scales in this problem, as suggested earlier in this section: a 'deterministic' time scale associated with the relaxation around each of the minima a and c, and a 'stochastic' one associated with transitions between a and c. The latter imply that: (i), a fluctuation has driven the system, initially on a or c, beyond the 'barrier' constituted by the unstable state b; and (ii), that the state reached in this way had the time to relax toward the new regime (respectively c or a) before a new fluctuation drove the system back to the basin of attraction of the original state.

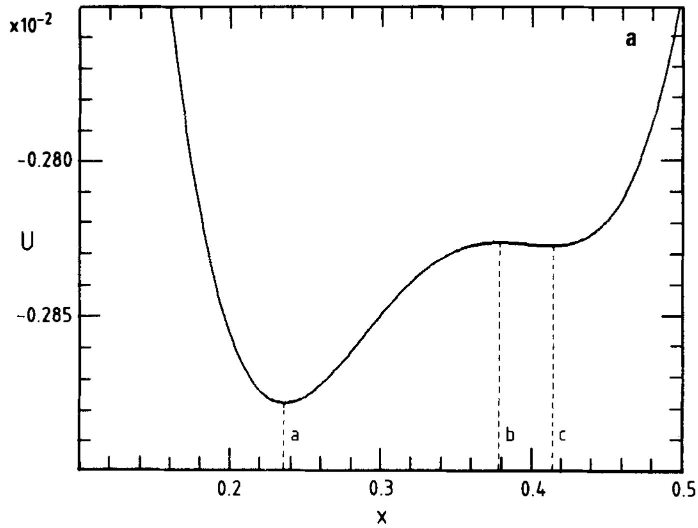

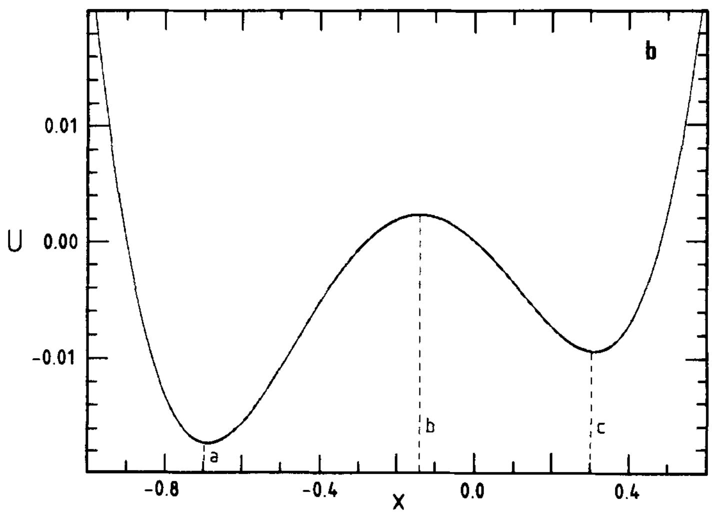

Figure 6. Bistable potential $U(x)$ as deduced from the model Eq. (16). (a) For the Kaédi station. (b) For Lamb's regional rainfall index. The difference between the value $U(a)$ and the maximum value $U(b)$ gives the magnitude of the barrier that the system must overcome before evolving to the high rainfall state c, starting from present state a.

Now, as seen in Fig. 6(a), the minimum associated with the state c of high rainfall is more shallow compared with the state a of low rainfall. This implies that $|U''(c)|$ and $|U''(b)|$ are very small or, alternatively (see Eq. (22)), that x evolves slowly near these states. This suggests that large excursions from c beyond the barrier may prove unsuccessful in bringing the system to state a, in the sense that the system will be driven back by a new fluctuation to c rather than evolve downhill to a. This mechanism of enhanced persistence is compatible with the large fluctuations around c observed in the record (see Fig. 1(a)). Conversely, large amplitude fluctuations around c imply a weakly stable state, and this should necessarily be reflected by a shallow minimum of the potential.

The above discussion allows us to justify and sharpen further the statement made at the beginning of the present section, that in the presence of only two, simultaneously stable states our cubic model contains all the dominant nonlinearities. Indeed, we saw that all relevant properties of our system are determined either by the local behaviour around a and c, or by the fluctuation-induced transitions between these states. Since the local behaviour is obtained by linearization around a and c, which are already given correctly by the cubic nonlinearities, higher-order terms will obviously be irrelevant in this respect. As regards the transition behaviour, we notice that it is conditioned by the structure and first few moments of the invariant probability distribution (Eq. (14a)). Now, as long as q^2 is reasonably small, these properties will be essentially given by the quartic part of $U(x)$, which is responsible for the double-well shape; all additional nonlinearities will give rise to contributions which vanish asymptotically with q^2 more quickly than the contributions coming from the quartic part.

Summarizing, then, one can assert that the model set forth in this paper is a canonical model capturing the essential features of the phenomenon of interest.

We close this section with a brief account of the modelling of the data pertaining to Lamb's regional precipitation index. Keeping again the dominant nonlinearities up to order three we obtain two stable states separated by an intermediate unstable one, and a double-well kinetic potential depicted in Fig. 6(b). The general shape of this potential is similar to the one of Fig. 6(a) obtained from the Kaédi data. The quantitative details are, on the other hand, different since in Lamb's regional index the variable is obtained from the original annual station precipitation amounts through a complex (nonlinear) normalization procedure, which changes completely the range of variation of the relevant properties. For this reason we restrict the quantitative part of the analysis of the next section to the Kaédi data only.

5. Transition time statistics

As already mentioned in section 4, in our model the dynamics is viewed as a succession of fluctuation-induced jumps. Moreover, because of the existence of the intermediate unstable state b, starting from a or c, a jump will not occur unless state b is reached through the jittery movement induced by the fluctuations. In this section we derive the characteristic times of these transitions. We first work with the dimensionless time τ, in order to obtain the relative properties of the two states independent of the specific value of ρ.

According to the theory of stochastic processes (Gardiner 1983) the mean time $\tau_1(x)$ for performing a transition between a and c is obtained in the following manner:

(i) Solve the following time-independent differential equation involving the adjoint Fokker–Planck operator:

$$A(x)d\tau_1/dx + \tfrac{1}{2}B(x)d^2\tau_1/dx^2 = -1 \tag{29a}$$

with

$$A(x) = f(x, \lambda_0), \qquad B(x) = q^2 \tag{29b}$$

and the following boundary conditions:

$$d\tau_1/dx = 0 \quad \text{at} \quad x = 0 \qquad \tau_1 = 0 \quad \text{at} \quad x = b \tag{30a}$$

for a transition from a to c via b, and

$$d\tau_1/dx = 0 \quad \text{at} \quad x = \infty \qquad \tau_1 = 0 \quad \text{at} \quad x = b \tag{30b}$$

for a transition from c to a via b.

(ii) Compute $\tau_1(x)$ successively for $x = a$ and for $x = c$. The result will represent half of the mean time needed to perform a transition from a to c or from c to a, respectively. The factor $\frac{1}{2}$ is due to the fact that once the system is on b, it has equal probability to go to either a or c.

We have solved Eqs. (29)–(30) numerically and obtained the following result:

$$\left.\begin{aligned} \tau_{1(a\to c)} &= 2\tau_{1(a\to b)} \approx 460 \text{ time units} \\ \tau_{1(c\to a)} &= 2\tau_{1(c\to b)} \approx 66 \text{ time units.} \end{aligned}\right\} \tag{31}$$

It seems therefore that the state of drought, a, has a greater persistence than the more favourable state, c, in agreement with the conclusions reached at the end of section 4 on the basis of the static properties. This prediction should, however, be dealt with with some caution. Indeed we have performed a more detailed analysis leading to the computation of the standard deviation, $\delta\tau_2$, and of the skewness, $\delta\tau_3$, around the above mean value τ_1. These quantities are defined by

$$\delta\tau_2 = (\tau_2 - \tau_1^2)^{1/2} \qquad \delta\tau_3 = (\tau_3 - 3\tau_2\tau_1 + 2\tau_1^3)^{1/3} \tag{32}$$

where τ_2, τ_3 obey the following equations:

$$A(x)d\tau_2/dx + \tfrac{1}{2}B(x)d^2\tau_2/dx^2 = -2\tau_1(x) \tag{33a}$$

and

$$A(x)d\tau_3/dx + \tfrac{1}{2}B(x)d^2\tau_3/dx^2 = -3\tau_2(x) \tag{33b}$$

and the same boundary conditions as in (30). Solving these equations numerically for the Kaédi data and substituting into (32) yields:

for the transition $a \to c$ via b:

$$\delta\tau_2 \approx 430 \text{ time units} \qquad \delta\tau_3 \approx 540 \text{ time units} \tag{34}$$

for the transition $c \to a$ via b:

$$\delta\tau_2 \approx 100 \text{ time units} \qquad \delta\tau_3 \approx 140 \text{ time units.} \tag{35}$$

We see that the system is characterized by a very pronounced variability, since the standard deviation is of the same order as the mean. Furthermore, because of the positive value of the skewness, the probability distribution of transition times is highly asymmetrical, its most probable value being shifted toward smaller values of the transition time relative to the mean.

Let us finally convert the above quantities to real-time units. Introducing the scale factor (see Eq. (28)) we obtain for the transitions $a \to c$ via b:

$$t_1 \approx 29\,\text{y};\ \delta t_2 \approx 27\,\text{y};\ \delta t_3 \approx 34\,\text{y} \tag{36}$$

and for the transition $c \to a$:

$$t_1 \approx 4\,\text{y};\ \delta t_2 \approx 6\,\text{y};\ \delta t_3 \approx 9\,\text{y.} \tag{37}$$

We must emphasize, however, that while the above values involve a certain amount of uncertainty due to the choice of a particular value of ρ, the *relative* stability of states a and c is independent of this choice. In addition, the strong variability of residence times appears to be an intrinsic property of the system.

Figure 7 depicts one particular realization of the stochastic process described by Eq. (19) obtained by numerical integration of this equation, using the parameter values of section 4 and an initial condition on state c. The simulation was performed for a time longer than the record available. We observe initially a high rainfall regime which persists

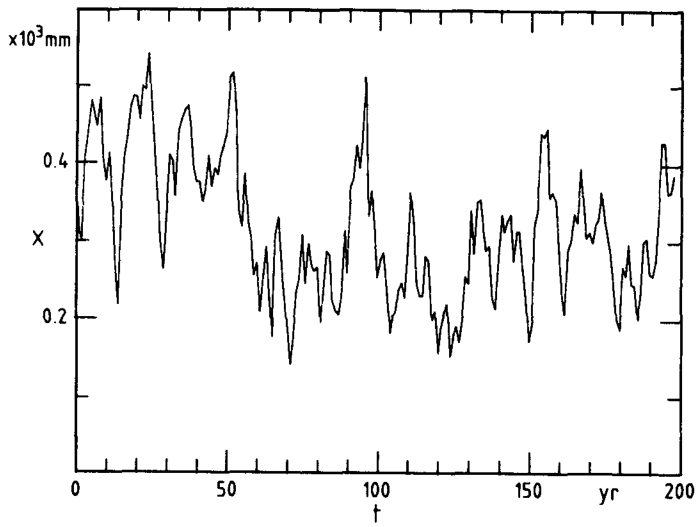

Figure 7. Typical time evolution of the variable x as given by the numerical integration of Eq. (19); $\tau = \rho t$ with $\rho \approx 16\,\mathrm{y}^{-1}$.

for about 50 years despite the small value of mean residence time of c. During this period the system performs large excursions to low values of x without falling into the attraction basin of a. Both properties are in agreement with our record and justify, *a posteriori*, the qualitative arguments advanced so far. Subsequently the system is caught into a low rainfall regime which persists over 30 years. The fluctuations around this latter regime are much smaller than around the previous one. This is again in agreement with the record. The simulation suggests that a short-lived high rainfall regime and a longer-lived low rainfall regime will follow successively. Notice the large difference of their persistence times compared with those of the first 80 years.

We emphasize that in addition to the realization depicted in Fig. 7 there exist many other realizations starting from the same initial condition. As a matter of fact the quantities evaluated previously, such as the mean residence times, can be understood as statistical averages over the ensemble of these realizations.

6. Conclusions

The data analysis and the mathematical modelling reported in this paper provide evidence that the Sahelian precipitation regime is not a random succession of dry and wet periods around a well-defined mean. Rather, we have shown that the salient features of the record can be accounted for by the following alternative: the system possesses two stable states of precipitation and switches back and forth between them as a result of the internal fluctuations or the external random perturbations to which it is inevitably subject. Despite the simplicity of the model developed it has been possible to reproduce some of the most conspicuous characteristics of rainfall in west Sahel, in particular abrupt changes in the precipitation regime of extremely variable duration (Nicholson 1989).

The most important consequence of the view advocated in the present work, is that instead of being completely elusive—as a noise-like process would be—the Sahelian precipitation regime enjoys some sort of predictability, at least in a statistical sense. In sections 4 and 5 we have computed a series of quantities corresponding to this prediction capability. We have seen that the low rainfall regime is both persistent and relatively predictable, a property which is in agreement with the rather small variability around the mean. On the other hand the quasi-normal rainfall has a much poorer predictability, as witnessed by the strong fluctuations around the mean. Thus, despite the rather small values of the mean residence time t_1 predicted by the model ($t_1 \approx 4\,\mathrm{y}$), such a regime can persist for much longer, as seen for instance in the particular realization depicted in Fig. 7. The historical record adds credence to this view.

The simplicity of the model used throughout our analysis and the limited number of data points entails some uncertainties as to the quantitative character of the results. We have emphasized that, despite such uncertainties, the model predictions on the *relative* properties of the two states of precipitation are likely to be robust.

We believe that the methods developed in the present paper lead to a new technique of data analysis that can be applied to other climatic phenomena likely to involve recurrent sharp transitions.

ACKNOWLEDGEMENTS

We are indebted to Dr R. Sneyers for enlightening discussions on the statistical analysis of the data and to an anonymous referee for constructive comments. Acknowledgement is made to Computational Mechanics Publications for the use of Figs. 1(b) and 2, to both the Data Bank Project, Programme Belgium–WMO (Brussels) and ASECNA (Nouakchott) for providing the precipitation data. The work of C. N. is supported, in part, by the European Economic Community under contract no. ST2J-0049-1-B(EBD).

REFERENCES

Box, G. E. P. and Jenkins, G. M. 1976 *Time series analysis, forecasting and control.* Holden-Day

Buishand, T. A. 1982 Some methods for testing the homogeneity of rainfall records. *J. Hydrol.* **58,** 11–27

1984 Tests for detecting a shift in the mean of hydrological time series. *ibid.*, **73,** 51–69

Bunting, A. H., Dennett, M. D., Elston, J. and Milford, J. R. 1976 Rainfall trends in the West African Sahel. *Q. J. R. Meteorol. Soc.*, **102,** 59–64

Charney, J. 1975 Dynamics of deserts and drought in the Sahel. *ibid.*, **101,** 193–202

Demarée, G. and Chadilly, M. S. 1988 The Sahelian drought(s) as seen from the rainfall data of a Mauritanian station. Pp. 15–23 in *Computer methods and water resources.* Vol. 3: *Computational hydrology.* D. Ouazar, C. A. Brebbia and V. de Kosinsky (Eds.) Computational Mechanics Publications and Springer-Verlag

Farmer, G. and Wigley, T. M. L. 1985 'Climatic trends for tropical Africa. A research report for the Overseas Development Administration'. Climatic Research Unit, University of East Anglia, Norwich

Folland, C. K., Palmer, T. N. and Parker, D. E. 1986 Sahel rainfall and worldwide sea temperatures, 1901–85. *Nature*, **320,** 602–607

Gardiner, C. W. 1983 *Handbook of stochastic methods.* Springer Verlag, Berlin

Glantz, M. and Katz, R. W. 1985 Drought as a constraint to development in sub-Saharan Africa. *Ambio*, **6,** 334–339

1986 African drought and its impacts: revived interest in a recurrent phenomenon. *Desertification Control Bulletin*, **14,** 22–30

Goossens, C. and Berger, A. 1987 How to recognize an abrupt climatic change? Pp. 31–45 in *Abrupt climatic change.* W. H. Berger and L. D. Labeyrie (Eds.) D. Reidel Pub. Company

Grove, A. T. 1973 A note on the remarkably low rainfall of the Sudan zone in 1913. *Savanna*, Vol. **2,** No. **2,** 133–138

Hare, F. K. 1983 *Climate and desertification: A revised analysis.* WCP-44, WMO/UNEP

Hasselmann, K. 1976 Stochastic climate models, Part I. Theory. *Tellus*, **28,** 473–485

Hubert, P. and Carbonnel, J. P. 1987 Approche statistique de l'aridification de l'Afrique de l'Ouest. *J. Hydrol.*, **95,** 165–183

Kendall, M. and Stuart, A. 1979 *The advanced theory of statistics*. Vol. 2 *Inference and relationship*. Ch. Griffin and Company Limited

Kraus, E. B. 1977 Subtropical droughts and cross-equatorial energy transports. *Mon. Weather Rev.*, **105**, 1009–1018

Lamb, P. J. 1982 Persistence of Subsaharan drought. *Nature*, **299**, 46–48

1983 Sub-Saharan rainfall update for 1982: continued drought. *J. Climatol.*, **3**, 419–422

1985 Rainfall in Subsaharan West Africa during 1941–1983. *Z. Gletscherk. Glazialgeo.*, **21**, 131–139

Landsberg, H. E. 1975 Sahel drought: Change of climate or part of climate? *Arch. Meteorol. Geoph. Biokl.*, Ser. B, **23**, 193–200

Nicholson, S. E. 1978 Climatic variations in the Sahel and other African regions during the past five centuries. *J. Arid Environ.*, **1**, 3–24

1989 Long term changes in African rainfall. *Weather*, **44**, 46–56

Nicholson, S. E. and Chervin, R. M. 1983 Recent rainfall fluctuations in Africa—Interhemispheric teleconnections. Pp. 221–238 in *Variations of the global water budget*. Alayne Street-Perrott, Mac Beran and Robert Ratcliffe (Eds). D. Reidel Pub. Company

Nicolis, C. 1988 Transient climatic response to increasing CO_2 concentration: some dynamical scenarios. *Tellus*, **40A**, 50–60

Nicolis, C. and Nicolis, G. 1981 Stochastic aspects of climatic transitions—Additive fluctuations. *ibid.*, **33**, 225–234

Nicolis, G. and Prigogine, I. 1977 *Self organization in non-equilibrium systems*. New York, Wiley

Oguntoyinbo, J. 1986 Drought prediction. Pp. 79–90 in *Climate and desertification*. J. P. van Ypersele and M. M. Verstraete (Guest Editors). *Climatic Change*, **9**

Otterman, J. 1974 Baring high albedo soils by overgrazing: A hypothetical desertification mechanism. *Science*, **186**, 531–533

Pettitt, A. N. 1979 A non-parametric approach to the change-point problem. *Appl. Statist.*, **28**, 126–135

Sircoulon, J. 1976 Les données hydropluviométriques de la sécheresse récente en Afrique intertropicale. Comparaison avec les sécheresses "1913" et "1940". *Cahiers ORSTOM, Série Hydrologique*, **XII**, 2, 75–174

Sneyers, R. 1975 'Sur l'analyse statistique des séries d'observations'. Note Technique No. 143, OMM-No. 415, Geneva

Snijders, T. A. B. 1986 Interstation correlations and nonstationarity of Burkina Faso rainfall. *J. Clim. Appl. Meteorol.*, **25**, 524–531

Sutera, A. 1981 On stochastic perturbation and long-term climate behaviour. *Q. J. R. Meteorol. Soc.*, **107**, 137–153